Received: 6 January 2023 | Revised: 31 August 2023 | Accepted: 6 September 2023

DOI: 10.1002/suco.202201227

ARTICLE

fib CEB-FIP WILEY

# 3D-printed concrete footbridges: An approach to assess the sustainability performance

**Javier Asensio**[1] | **Irene Josa**[2] | **Andrea Monserrat**[3] | **Albert de la Fuente**[4]

[1]WMM Ingenieure AG, Münchenstein, Switzerland

[2]Department of Civil, Environmental & Geomatic Engineering, University College London, London, UK

[3]School of Civil Engineering. Universidad Politécnica de Madrid (UPM), Madrid, Spain

[4]Department of Civil and Environmental Engineering, Universitat Politècnica de Catalunya (UPC), Barcelona, Spain

**Correspondence**

Albert de la Fuente, Department of Civil and Environmental Engineering, Universitat Politècnica de Catalunya (UPC), Barcelona, Spain.

Email: albert.de.la.fuente@upc.edu

**Funding information**

ACCIONA; Ministerio de Ciencia, Innovación y Universidades; Ministerio de Universidades; Universitat Politècnica de València

**Abstract**

Digital fabrication with concrete (DFC) is fast becoming an attractive alternative for components (i.e., façades, urban furniture) and structural typologies (i.e., short-span footbridges, columns, floor systems) for which complex geometries derived from particular aesthetical criteria and/or construction time constrictions are governing parameters. Additionally, some authors claim that this process allows improving the sustainability of structures, as less material is necessary compared to traditional concrete solutions, thus reducing greenhouse gas emissions linked to material consumption. Nonetheless, the environmental implications of DFC are still under scrutiny and remain objectively unquantified. In this study, a sustainability assessment model to allow decision-makers to evaluate and compare concrete footbridge alternatives—from the sustainability perspective—including those constructed by means of 3D printed concrete (3DPC) techniques, is presented. The proposed approach is based on the MIVES method. For this purpose, the most representative criteria and indicators of sustainability identified are measured and weighted-aggregated in a decision-making tree. The sustainability index (SI) of each alternative is the outcome derived from the application of the model, and the SI was used as reference for evaluating the alternatives. The sustainability of 3D-printed footbridges is quantified and compared to other concrete-based solutions: traditional reinforced cast-in-place and precast concrete, as traditional solutions, and ultra-high performance precast concrete and textile-reinforced concrete, as innovative alternatives. The results of the analysis lead to conclude that 3D-printed footbridges have positive impacts on environmental and social indicators, but economic indicators still need to be improved to attain a competitive solution. The approach proposed herein to assess the sustainability of footbridges can be extended to other cases and stakeholders' preferences by adapting the components of the method to sensitivities and particular boundary conditions of other scenarios.

**KEYWORDS**

3D printed concrete (3DPC), digital fabrication with concrete (DFC), footbridge, life cycle assessment, sustainability

## 1 | INTRODUCTION

In recent years, digital fabrication with concrete (DFC) has generated large interest in the construction sector, especially in architectural environments.[1] While originally developed for improving productivity issues in construction,[2] DFC has undergone comprehensive exploration across diverse dimensions in the last few years, such as process optimization,[3] material advancements,[4,5] and structural innovations.[6,7]

It is important to clarify that, from the authors' perspective, DFC methods are not intended (and should not be expected) to cover universal applications, but rather find valuable utility in specific structural elements. In this context, different additive manufacturing (AM) processes can be used for DFC in the construction sector. A classification of the different processes was proposed by Buswell et al.[8] based on seminal work from the RILEM technical committee 276-DFC on "Digital fabrication with cement-based materials." According to this, three groups can be distinguished depending on the deposition system of the cement-based materials: particle bed binding, material extrusion, and material jetting (Figure 1). In light of the scientific production related to AM, it can be stated that extrusion-based processes, such as contour crafting (CC) or concrete printing (CP), have aroused more interest than particle bed 3D printing systems.[12]

CC[13] is based on an extrusion and filling process that allows moving the printing nozzle through a mechanized gantry system—movement along axes X and Z—and a sliding structure—movement along axe Y. Along with these movements, the rotation of the nozzle on its own axis makes up a 4-degree-of-freedom system. Regarding CP,[14,15] although it was also developed as a system with 4 degrees of freedom thanks to the swivel head installed on the mechanized gantry system—movement along axes X, Y, and Z, this initial development has been replaced by the 6-degree-of-freedom articulated robotic arm. These two techniques, CC and CP, allow printing parallel and uniform layers of cementitious material, being suitable for the manufacture of elements such as house walls.

Regarding particle bed 3D printing systems, Lowke et al.[16,17] identified three types, namely selective binder

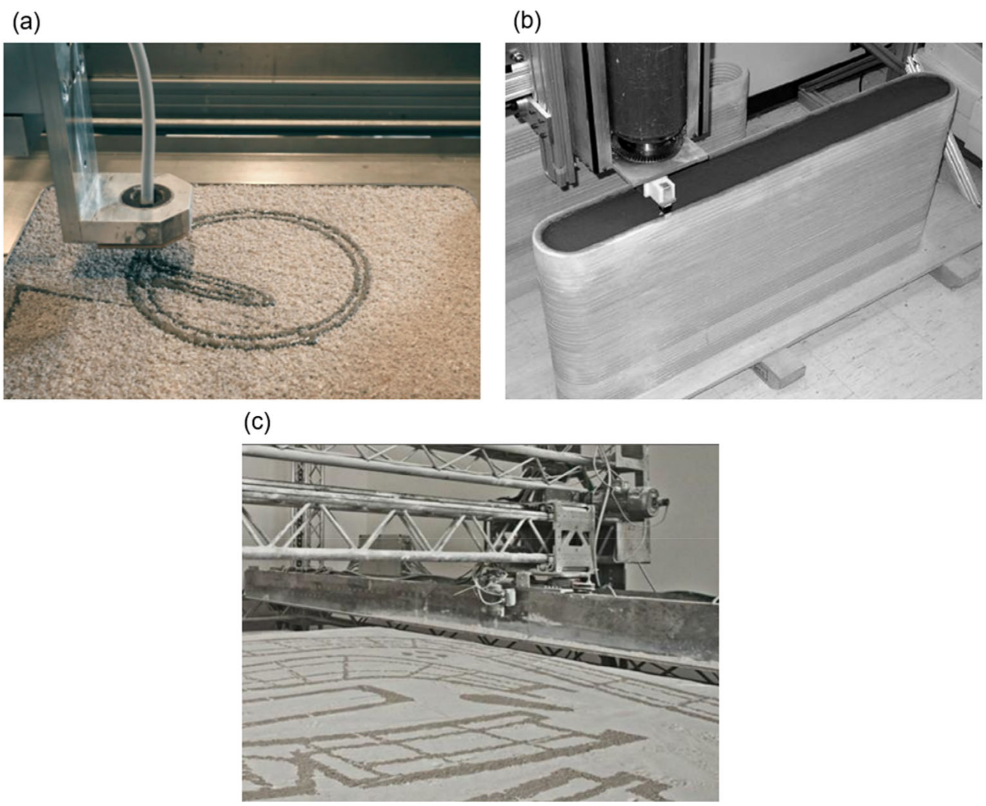


FIGURE 1 Examples of different cement 3D printing systems, including (a) particle bed binding (credit[9]), (b) material extrusion (credit[10]), and (c) material jetting (credit[11]).

activation type,[18] selective paste intrusion type,[19] and binder jetting type.[20] One of the most common particle bed binding systems is D-Shape. This is a selective binder activation technique,[16] since the cement of a dry mix (fine aggregate and cement) is activated with a water solution in defined areas thus generating a cement-based plaster around the aggregates. The system requires several spray nozzles that are installed on a mechanized beam—movement along axes X and Y—connected to a rectangular frame—movement along axe Z.[21]

Some of the main advantages of DFC include the design freedom of complex geometries and shapes due to the lack of need for formwork, the reduction of the construction time, which is particularly important for elements with complex geometries, and the reduction in labor and material costs.[22] In addition, DFC allows parametric design and topological optimization of concrete sections, which results in a reduction of the cementitious material. In fact, in some structures such as 3D printed concrete (3DPC) footbridges, material savings arising from the use of DFC are reported to reach up to 30% and $CO_2$ emissions can be reduced by up to 40% compared to traditional concrete solutions (see, e.g., the 3DPC footbridge in Zhaozhou, China, or the one located in Aubervilliers, France).[23,24]

Considering that cement production is the main source of greenhouse gas emissions into the atmosphere, the consumption of less material by elements built with DFC has been claimed by some authors to enhance the environmental footprint of the construction sector by a direct reduction of emissions of polluting gases.[25] Nonetheless, the benefits and drawbacks that exist in terms of sustainability impacts of elements produced with DFC are still subjected to analysis and discussion. In this regard, the higher content of binder necessary to make the mix pumpable[26] is one of the aspects that negatively impacts the sustainability performance—specially the economic and environmental indicators—of DFC. In this context, Flatt and Wangler[1] claimed that the environmental footprint of DFC is higher than that of conventional concrete due to aspects such as overdesign of strength. This increase of strength respect to that derived from the design, although unnecessary from the strict mechanical performance requirements, is often imposed to cover other uncertainties (i.e., potential spatial heterogeneity of the mechanical properties of the material owe to fabrication process, geometric tolerances, among others) that have an impact of the structural reliability. This increase of mechanical performance leads to reasonable safety margins required for new—still under development—materials and construction technologies.[27]

Hence, in order to make informed decisions that place sustainability at their core, it is essential that practitioners and stakeholders have tools to select sustainable solutions, both considering conventional and DFC alternatives. Therefore, the objective of this paper is to provide designers with a tool that enables assessing the sustainability performance of construction and materials' technologies—covering conventional and innovative technologies. In this study, this approach is based on an identification of the most representative criteria and indicators of sustainability. In particularly, economic, environmental and social pillars were involved and, through combining those and resorting to the concept of value/satisfaction function, a sustainability index (SI) of each alternative under analysis can be derived by using MIVES (from Spanish "Modelo Integrado de Valor para Evaluaciones Sostenibles," and translated to Integrated Value Model for Sustainable Evaluations).[28,29]

The MIVES model has been satisfactorily used for quantifying sustainability in other fields of engineering such as *underground*,[30–32] *hydraulic*,[33–35]*electric-power generation infrastructures*,[31,36] *building*,[29,37–42] and *post-disaster re-construction*.[43,44] A number of researchers[45,46] have also developed methods intended to treat the uncertainties related to the input data.

Considering (1) the rapidly growing number of 3DPC footbridges built over the last decade and (2) the need of embedding the sustainability quantification in the decision-making process during the conceptual design phase—for all the material and structural typologies subjected to analysis-, this paper uses 3DPC footbridges as case study. In the following section, the state-of-art of 3DPC footbridges is presented, and the most important examples to date are described. Then, the methodology of the study is presented in Section 3, followed by a discussion of the results (Section 4), and the conclusions (Section 5).

## 2 | STATE-OF-ART OF 3DPC FOOTBRIDGES

So far, the construction of 3DPC footbridges has involved both CP and D-Shape techniques. Existing examples of already built footbridges include four arch footbridges—located in Alcobendas (Spain), Shanghai (China), Tianjin (China), and Venice (Italy)—and three beam footbridges—located in Gemert, Nijmegen, and N243 route (Holland). Table 1 summarizes the main information related to the projects of these footbridges, and Figure 2 provides their graphical representation.

The footbridge Parque de Castilla in Alcobendas (Spain, 2016, see Figure 2a) was the first 3DPC footbridge of the world[27] produced with the D-Shape technology. It is a pedestrian single arch footbridge of 12.0 m span and

TABLE 1 3DPC footbridge projects executed.

| Project | Location | Opening year | Length (m) × width (m) | Span (m) | Designer | Construction company | AM process | Typology |
|---|---|---|---|---|---|---|---|---|
| Footbridge "Parque de Castilla" | Alcobendas (Spain) | 2016 | 12.0 × 1.75 | 12.0 | ACCIONA (ES). IAAC (ES). UPC (ES) | Acciona (ES). D-Shape (IT) | D-Shape | Arch |
| Footbridge Gemert | Gemert (Holland) | 2017 | 8.0 × 3.5 | 8.0 | Witteveen+Bos (NL). TU/e (NL) | BAM Infra (NL). Weber Beamix (NL) | CP | Beam |
| Footbridge "Wisdom Bay Park" | Shanghai (China) | 2019 | 26.3 × 3.6 | 14.4 | Tsinghua University (CN) | Unknown | CP | Arch |
| Footbridge Zhaozhou | Tianjin (China) | 2019 | 28.1 × 4.2 | 17.9 | Hebei University of Technology (CN) | Hebei University of Technology (CN) | CP | Arch |
| Striatus | Venice (Italy) | 2021 | 16.0 × 12.0 | 15.1 | BRG (CH). ZHACODE (UK) | Incremental3D (AT). Holcim | CP | Arch |
| The Bridge Project | Nijmegen (Holland) | 2021 | 29.5 × 3.6 | 5.7 | Michiel van der Kley (NL). Witteveen+Bos (NL). TU/e (NL) | BAM Infra (NL). Weber Beamix (NL) | CP | Beam |
| Footbridges of N243 route | N243 (Holland) | N/A | 12.0 × 4.5 | 11.0 | Witteveen+Bos (NL). TU/e (NL) | BAM Infra (NL). Weber Beamix (NL) | CP | Beam |

U-shaped section of 1.75 m width. The cement-based composite used was reinforced with steel micro-fibers (1.3% in volume) for cracking control purposes. The structure is composed of eight individual segments that were assembled above a steel curve frame—finally integrated in the footbridge—resulting in a 15.0 t footbridge. Regarding the steel substructure, although its structural contribution was disregarded in both service and ultimate limit states, it is meant to guarantee the required stability and bearing capacity of the footbridge in the accidental event in which the 3DP cement-based material would suffer from any unexpected (and unknown) degradation mechanism.

Also, at the forefront, is the bicycle footbridge constructed in the ring road of Gemert (Holland, 2017, see Figure 2b), as it is the first post-tensioned 3DPC footbridge of the world.[47,48] It is a beam structure of 8.0 m span and 3.50 m width composed by six segments of 0.92 m height fabricated with cementitious composite using CP technique. Besides the unbonded post-tensioning designed to ensure no tension stresses at any cross-section of the footbridge and also no opening of the joints between adjacent segments—even for ultimate limit state load combinations, a high-performance steel cable was embedded within the 3D-printed mortar filament—during the precast process—to prevent the deck from a potential brittle failure, this cable acting both as a shear reinforcement and as a confining element.

Another pedestrian 3DPC footbridge was constructed in Wisdom Bay Industrial Park in Shanghai (China, 2019, see Figure 2c) using the CP technique.[49] The cement mortar was reinforced with polyethylene fibers. The footbridge consists of a square-section single arch of 26.3 m length (14.4 m span) and 3.6 m width composed by 44 segments. In addition to these segments, 68 more were used for the parapet and 64 for the pavement. This is a case of a composite 3D concrete-steel footbridge, where both concrete and steel work as load-bearing elements.

The 3DPC pedestrian footbridge with the longest span—17.9 m—of the world (arch of 28.1 m length and 4.2 m width) is located in Tianjin (China, 2019, see Figure 2d). It was constructed as a replica of the most ancient bridge in China, the arch stone bridge Zhaozhou. The available information of the project indicates that the structure was fabricated with fiber-reinforced cement mortar (CP technique) and it was assembled through post-tensioned bars. Thus, the 3D-printed concrete is the element assigned with the structural mission of bearing the service load.


**FIGURE 2** 3DPC footbridge projects: (a) Parque de Castilla (credit: Institute for Advanced Architecture of Catalonia, IAAC); (b) Gemert (credit: Marc Zoutendijk); (c) Wisdom Bay Park (credit: Tsinghua University); (d) Zhaozhou (credit: Xinhua); (e) Striatus (credit: naaro); (f) The Bridge Project (credit: Municipality of Nijmegen); and (g) N243 route (credit: Witteveen+Bos).

In Innsbruck, a pedestrian arch footbridge was precast by means of the incremental 3D (in3D). The structure is placed in Venice (Italy, 2021, see Figure 2e), and it is known as Striatus. The arch is 16 m long and 12 m wide—15.1 m span—and it is composed by 53 alveolar segments of variable section and length printed in 3D using CP technique. While the concrete is bearing the major load in this structure, there are tie bars designed to absorb horizontal loads resulting from the static equilibrium at the foundations and to avoid its transfer to the soil.

The longest 3DPC (CP technique) footbridge in the world (29.5 m length and 3.6 m width) was constructed in the Geologenstrook park in Nijmegen (Holland, 2021, see Figure 2f)[14] for cycling use. The beam footbridge is divided into five spans—5.7 m span length—and it is supported by eight intermediate piers—also 3D printed. The structure is composed by 46 post-tensioned alveolar segments along the deck and U-shaped sections filled with conventional concrete on supports (piers and abutments). This structure uses the same structural technique as the footbridge in Gemert, as the design team was the same.

Finally, there are four bicycle footbridges projects in the N243 route between Schermerhorn and Noordbeemster (Holland, 2022, see Figure 2g), whose construction is by means of 3DPC using CP technique. All of them are beam footbridges composed by six segments with post-tensioned hollow-core box section and are 12.0 m long and 4.5 m wide —11.0 m span. Again, these footbridges applied a similar technique as that one in Gemert.

These short-span 3DPC footbridges constructed—and others currently under design—allow confirming both the technical and scientific interest of stakeholders in this technique. So far, the analyses carried out consisted in material and structural studies required to guarantee success of these pilots as well as economic studies aimed at comparing the traditional construction techniques with the 3DPC alternatives constructed. Nonetheless, an objective and integrated sustainability assessment (accounting for economic, environmental, and social indicators) comparing the most representative alternatives (based on the use of cement-based materials) is still to be carried out and the results to be subjected to discussion.

## 3 | METHODOLOGY

This section introduces the methodology used to assess the sustainability of short-span concrete footbridges. First, the method MIVES is described, followed by the sustainability assessment model developed.

### 3.1 | Introduction to MIVES

The methodology MIVES is a multi-criteria decision-making methodology that evaluates each of the alternatives within a specific problem through a sustainability index (SI). This SI is obtained as a weighted sum of the valuations of the different criteria and indicators considered. While details on this methodology can be found elsewhere (i.e., References 28,29), its main phases are briefly introduced below.

1. Identification and delimitation of the decision/s to be made. The objective and system boundaries are defined.
2. Definition of the decision tree. The decision tree is a structured representation of the criteria and indicators that will be analyzed. In the first level of the three, the sustainability requirements/pillars are identified (i.e., economic, environmental, social). In the second level, the criteria are more concrete groups of the attributes that will be assessed. Finally, the third level, which contains indicators, comprises the most specific metrics that will be quantified. A generic example of the decision tree is shown in Figure 3.
3. Generation of value functions. Given that each indicator may have different units, a normalization process is necessary to transform all the variables into the same range (namely, between 0 and 1 for the minimum and maximum satisfaction, respectively). The value functions are used to perform such normalization, and they allow transforming the raw data using different shapes. These different shapes can be linear, concave up, concave down, and S-shaped.
The value functions are obtained using Equations (1) and (2), where $X_i$ is the value of the data for the indicator assessed, $C_i$ is approximately the inflection point on the x-axis, $K_i$ is approximately the y-value of the inflection point, and $P_i$ is a factor that defines the shape of the graph.

$$V_{ind} = B \cdot \left[1 - e^{-K_i \left(\frac{|X_i - X_{min}|}{C_i}\right)^{P_i}}\right] \tag{1}$$

$$B = \left[1 - e^{-K_i \left(\frac{|X_{max} - X_{min}|}{C_i}\right)^{P_i}}\right]^{-1} \tag{2}$$

4. Allocation of weights. Weights are necessary to aggregate the indicators into a single sustainability index. There are different ways in which weights can be allocated, such as direct allocation, or through the analytical hierarchy process (AHP).
5. Evaluation of the alternatives. The evaluation of the alternatives is obtained after assessing indicators, criteria, and requirements.

### 3.2 | Decision model

The decision-making model used in this study was developed based on decision-making trees proposed by various authors. A number of pertinent studies were carefully chosen, and the weights assigned to the requirements, criteria, and indicators were extracted from the decision-making trees employed in these studies. Specifically, decision trees for train bridges,[50] concrete piles,[51] sport hall roofs,[29] pre-cast concrete,[52] concrete tunnels,[33,34] and wind turbines[53] were selected due to their relevance to infrastructure. To determine the sets of weights for requirements, criteria, and indicators, both the mean and variance were calculated. These findings have been included in Tables A1, A2, and A3, respectively, which can be found in the Appendix.

For the final definition of the decision-making tree (see Table 2), the following considerations were made:

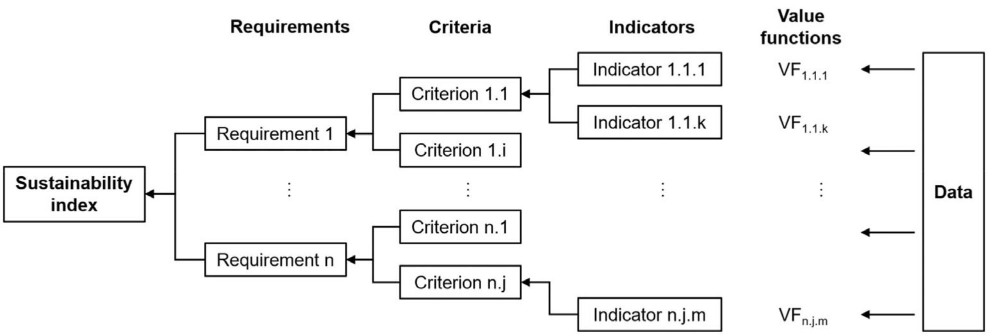


FIGURE 3 Representation of a generic decision tree as defined in MIVES.

- In assigning weights to the requirements, the economic, environmental, and social pillars were considered, and the mean weights from Table A1 were used. This approach was considered to provide a representative view of the importance associated to each component. It is worth noting that in different contexts, alternative sets of weights can be considered without compromising the validity and robustness of the sustainability analysis presented in this study.
- The criteria selected were those with a mean weight equal to or greater than 10% of the total weight, as indicated in Table A2. Based on this hypothesis, the following considerations were made: (1) selecting indicators that are representative and whose variability could potentially influence the calculated SI; (2) streamlining the assessment process, particularly the quantification phase of the indicators, to make it less time-consuming and more accessible to end users who may not be familiar with this type of assessment; and (3) ensuring the representativeness and satisfactory accuracy of the SI derived.
- In selecting the indicators, those with a mean weight exceeding 5% were chosen, following the same rationale applied to the criteria (see Table A3). However, the maintenance costs indicator, despite having a mean weight higher than 5%, was not included in the analysis due to the following reasons: (1) to minimize maintenance costs, with measures such as sufficient concrete cover for reinforcement and water/cement ratios ensuring the service life required in the project, and (2), there is no reliable data regarding some of the alternatives in relation with the maintenance costs. The indicator *water consumption* (related to materials extraction/treatment and construction) was implicitly incorporated within the indicator for *materials consumption*. Lastly, the indicator for *local nuisances*, encompassing aspects like noise pollution, particle pollution, traffic disruptions, space occupancy during construction, and user comfort, was included with a weight of approximately 8%.

In the decision-making tree defined (Table 2), the first requirement ($R_1$) encompasses one criterion ($C_1$, *costs*), and one indicator ($I_1$, *construction costs*). This indicator incorporates all costs from phases A1 to A5, spanning from the initial stages to practical completion, as defined in EN-15978 for lifecycle assessment. Therefore, the costs included are the material supply, equipment, and manpower for the production and assembly of the infrastructure, as well as the transportation and the commissioning of the footbridge. A decreasing S-shaped value function was defined for this indicator.

The *environmental requirement* ($R_2$) contains three distinct criteria (i.e., $C_2$, *resource consumption*, $C_3$, *energy consumption*, and $C_4$, *emissions*). Each criterion is represented by a single indicator. The same value function, a decreasing concave function, was assigned to all three indicators.

Lastly, the *social requirement* ($R_3$) is measured through two criteria ($C_5$, *working conditions*, and $C_6$, *third party effects*), each having one associated indicator. Indicator $I_5$, *Occupation Risk Index* (ORI) evaluates the degree of health and safety hazards faced by workers, and it depends on the volume and type of activities carried out.[54] For this indicator, a decreasing linear function was defined.

The last indicator ($I_6$, *local nuisances*) considers the inconveniences experienced by the local community due to land use, noise and dust generation, and changes in traffic patterns. the qualitative scale established for the assessment of this indicator can be found in Table A4.

The parameters that were used to define the value functions for each of the indicators described above are presented in Table 3. Their graphical representation has been included in the Figure A1.

## 4 | STUDY CASE

The study case aims to evaluate and compare the sustainability of different solutions of concrete footbridges—including the 3DPC alternative—based on the decision-

TABLE 2 Proposed decision-making tree.

| Requirements | | | Criteria | | | Indicators | |
|---|---|---|---|---|---|---|---|
| $R_1$ | Economic | 40% | $C_1$ | Costs | 100% | $I_1$ | Construction costs |
| $R_2$ | Environmental | 40% | $C_2$ | Resource consumption | 37.5% | $I_2$ | Material consumption |
| | | | $C_3$ | Energy consumption | 25% | $I_3$ | Energy consumption |
| | | | $C_4$ | Emissions | 37.5% | $I_4$ | $CO_2$ emissions |
| $R_3$ | Social | 20% | $C_5$ | Working conditions | 70% | $I_5$ | ORI |
| | | | $C_6$ | Third party effects | 30% | $I_6$ | Local nuisances |

TABLE 3 Parameters used for the value functions of the indicators.

| | | | MIVES parameters | | | | |
|---|---|---|---|---|---|---|---|
| Indicator | | Unit | Min | Max | *C* | *K* | *P* |
| 1 | Construction costs | € | 0.5 | 3 | 2.2 | 2 | 2.5 |
| 2 | Material consumption | t | 0.25 | 1.25 | 1.2 | 2.9 | 1 |
| 3 | Energy consumption | MJ | 0.25 | 1.25 | 1.2 | 2.9 | 1 |
| 4 | $CO_2$ emissions | kg $CO_2$-eq | 0.25 | 1.25 | 1.2 | 2.9 | 1 |
| 5 | ORI | - | 0 | 2.5 | 1.2 | 0 | 1 |
| 6 | Local nuisances | - | 1 | 0 | 1.2 | 0 | 1 |

making tree presented in Table 2. All alternatives were designed to cover a free span of 12.0 m and to serve exclusively as platform for pedestrians and bicycles according to Eurocode 2.[55] The exposure conditions are normal, and the existence of aggressive agents (chlorides, acids, and other substances) and other extreme exposure conditions that could reduce the service life of the structure were unconsidered.

In this section, the details of the alternatives analyzed are presented. These include a digitally constructed solution (3D-printed concrete), two traditional solutions (cast-in-place concrete and precast concrete), and two innovative solutions (precast ultra-high performance concrete and textile reinforced concrete).

## 4.1 | Alternatives

The five solutions that were defined for the analysis are the ones described below and represented in Figure 4. The acronym that will be used for each alternative in the following sections is shown in brackets.

- Cast-in-place reinforced concrete footbridge (REF). This is a traditional solution both in terms of materials and constructive process, and it is considered in this study as the reference solution. Its details are represented in Figure 4a.
- 3DPC footbridge (3DPC). The Parque de Castilla footbridge already constructed in Alcobendas, in Spain, ([27]; Institute for advance architecture of Catalonia [IAAC],[56]) is considered in this solution. It is shown in Figure 4b. Constructor and owner of the 3D printer being ACCIONA, Ltd.
- Precast concrete truss footbridge (TRS). This alternative is an evolution of the REF solution to reduce the concrete volume and based on the geometry and constructive process of the Barranco de las Ovejas footbridge located in Alicante, in Spain.[57] It is represented in Figure 4c.
- Precast ultra-high-performance concrete footbridge (UHPC). It is an innovative solution based on the Bouveret footbridge in Port-Valais, in Switzerland.[58,59] It is shown in Figure 4d.
- Precast textile-reinforced concrete footbridge (TRC). This is an innovative solution to optimize the concrete volume and based on the Albstadt-Ebingen footbridge in Germany.[60,61] It is shown in Figure 4e.

Note that, among the different alternatives, the only really executed solution is the 3DPC Parque de Castilla footbridge (Spain, 2016), the other four designs are close to usual practice—even inspired by real designs but not really constructed (and even not considered into decision-making analysis by the constructor as the objective was to construct a 3PDC solution).

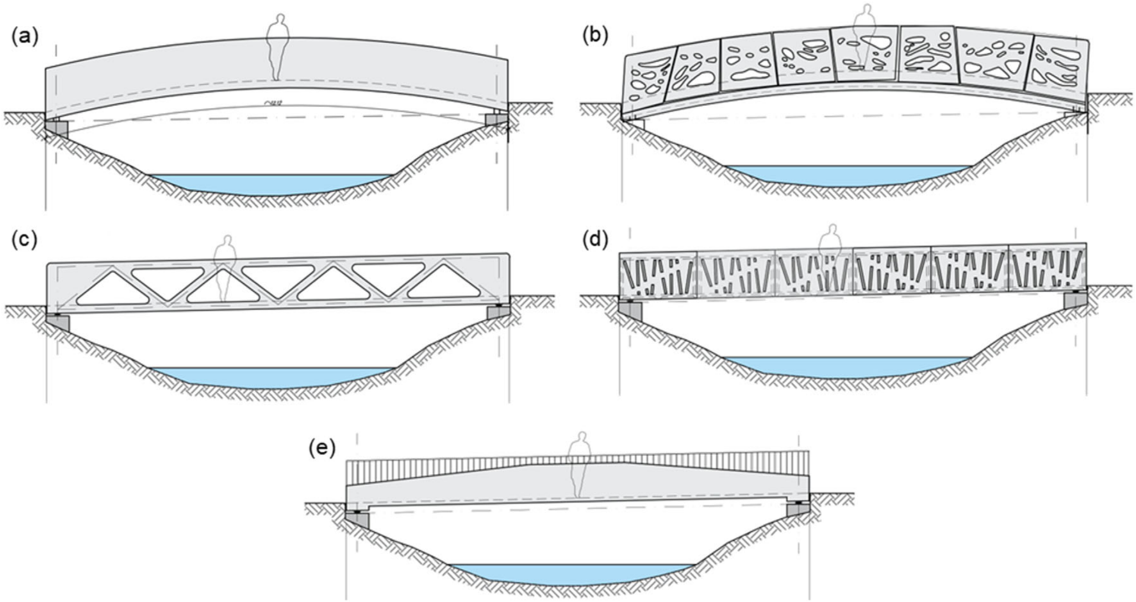


**FIGURE 4** Footbridges solutions analyzed in the study case: (a) REF; (b) 3DPC; (c) TRS; (d) UHPC; and (e) TRC.

**TABLE 4** Geometrical definition of the five alternatives for the footbridges.

| Solution | $b_1$ (m) | $b_2$ (cm) | $h_1$ (m) | $h_2$ (cm) | Number of segments |
|---|---|---|---|---|---|
| REF | 1.60 | 20 | 1.30 | 20 | - |
| 3DPC | 1.75 | 27 | 1.38 | 28 | 8 |
| TRS | 1.60 | 20 | 1.30 | 20 | - |
| UHPC[a] | 1.40 | 5 | 1.24 | 5 | 6 |
| TRC[b] | 1.34 | 7 | 0.65/0.99 | 20/9 | - |

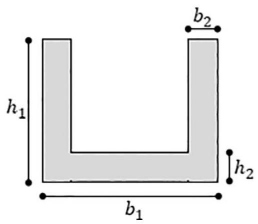


[a]Post-tensioned footbridge: horizontal tendons along the parapets and the deck.
[b]Variable depth footbridge with variable height of the parapets (*support section/mid-span section*).

### 4.1.1 | Geometry

All the proposed solutions have the same geometrical conditions as the 3DPC solution, this being a footbridge already executed.[27,56] Therefore, the five footbridges have a 12.0 m span and a U-shaped section of 1.2 m useful width.

Table 4 summarizes the footbridge section for the five solutions and the mid-span sections of these solutions are shown in Figure 5. Related to the geometry presented in Table 4, the UHPC solution is designed with horizontal post-tensioned tendons along the parapets and deck, the section having a greater thickness at this area to ensure the force transmission—$b_2 = 0.10$ m and $h_2 = 0.14$ m. Moreover, the TRC solution is a variable depth footbridge with parapets of variable height too, ensuring a lateral height of 1.1 m by means of a railing along the entire footbridge.

Regarding Figure 5, the color pattern used is intended to distinguish between printed areas (dark gray) and voids or non-printed areas (light gray), which are meant to reduce the weight of the structure and the material consumption, while guaranteeing the targeted bearing capacity. In Figure 5b, the height of the printed layers was 5 mm, compatible with the maximum aggregate size (5 mm) used in the mortar composition.

### 4.1.2 | Materials

Table 5 presents the concrete mix design for the various footbridge solutions, as well as the total concrete volume employed in each one. In all cases, the cement is CEM I 52,5 and the density of the mix considering all the materials included in Table 5 is 2500 kg/m$^3$.

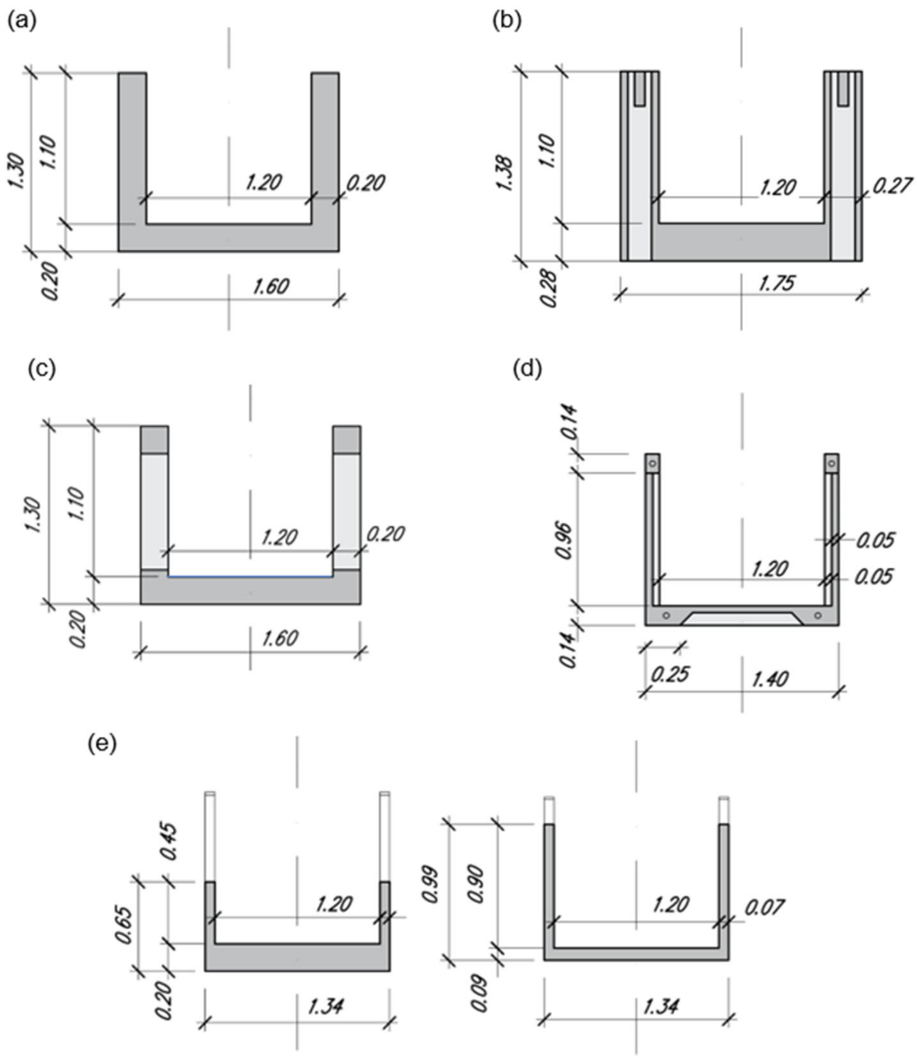


**FIGURE 5** Representation of the mid-span section for the five alternatives for the footbridges: (a) REF; (b) 3DPC; (c) TRS; (d) UHPC; and (e) TRC (mid-span section and support section). Measurements are shown in meters.

**TABLE 5** Concrete mix design for the five alternatives for the footbridges.

| Solution | Cement (kg/m$^3$) | Aggregates [$d_g$ in mm] (kg/m$^3$) | Water (kg/m$^3$) | Reinforcement (kg/m$^3$) | Additives (kg/m$^3$) | Concrete volume (m$^3$) | References |
|---|---|---|---|---|---|---|---|
| REF | 275 | 1845 [20] | 165 | 150 (steel B500S) | 65 | 9.12 | Concrete C 30/37[62] |
| 3DPC | 500 | 200 [1] /1250 [2] | 210 | 100 (steel micro-fibers) | (Not defined—Unknown) | 6.00 | Provided by company |
| TRS | 315 | 1770 [12] | 165 | 200 (steel B500S) | 50 | 5.96 | Concrete C 35/45[63] |
| UHPC | 750 | 1320 [–] | 150 | 75/75 (steel fibers/steel B500S) | (Not defined—Unknown) | 3.05 | Based on Ductal © concrete (Holcim product) |
| TRC | 500 | 1800 [5] | 150 | 10/- (carbon fibers/textile mesh) | 50 | 2.51 | Concrete C 50/60[64] |

Both the REF and the TRS alternatives consider traditional reinforced concrete, with a characteristic compressive strength of 30 and 35 MPa, respectively. In the case of the 3DPC solution, the material employed was steel fiber-reinforced concrete (SFRC)—100 kg/m$^3$ of steel micro-fibers 13.0 mm long and 0.15 mm diameter.[27] For the UHPC solution, a SFRC mix based on the Bouveret footbridge[59]—75 kg/m$^3$ of steel fibers, compressive strength between 150 and 180 MPa—along with post-tensioning tendons are proposed. Finally, self-compacting carbon fiber-reinforced concrete—10 kg/m$^3$ of carbon fibers, compressive strength of 60 MPa—based on the Albstadt-Ebingen footbridge[61] is proposed for the TRC solution. In this case, in addition to fibers, textile mesh reinforcement consisting of fiber roving arranged in two directions is also considered.

### 4.1.3 | Structural design

For the structural design of all the alternatives, AxisVM-X6 finite element software (developed by the Hungarian company Software Development Company) was used. In addition to the self-weight of the footbridge, 2 kN/m$^2$ of dead load and 5 kN/m$^2$ of live load were considered in the analysis. It must be pointed out that the 3DPC alternative was not analyzed with the software. It is the only footbridge already executed and its dimensions and boundary conditions provided the basis for the design of

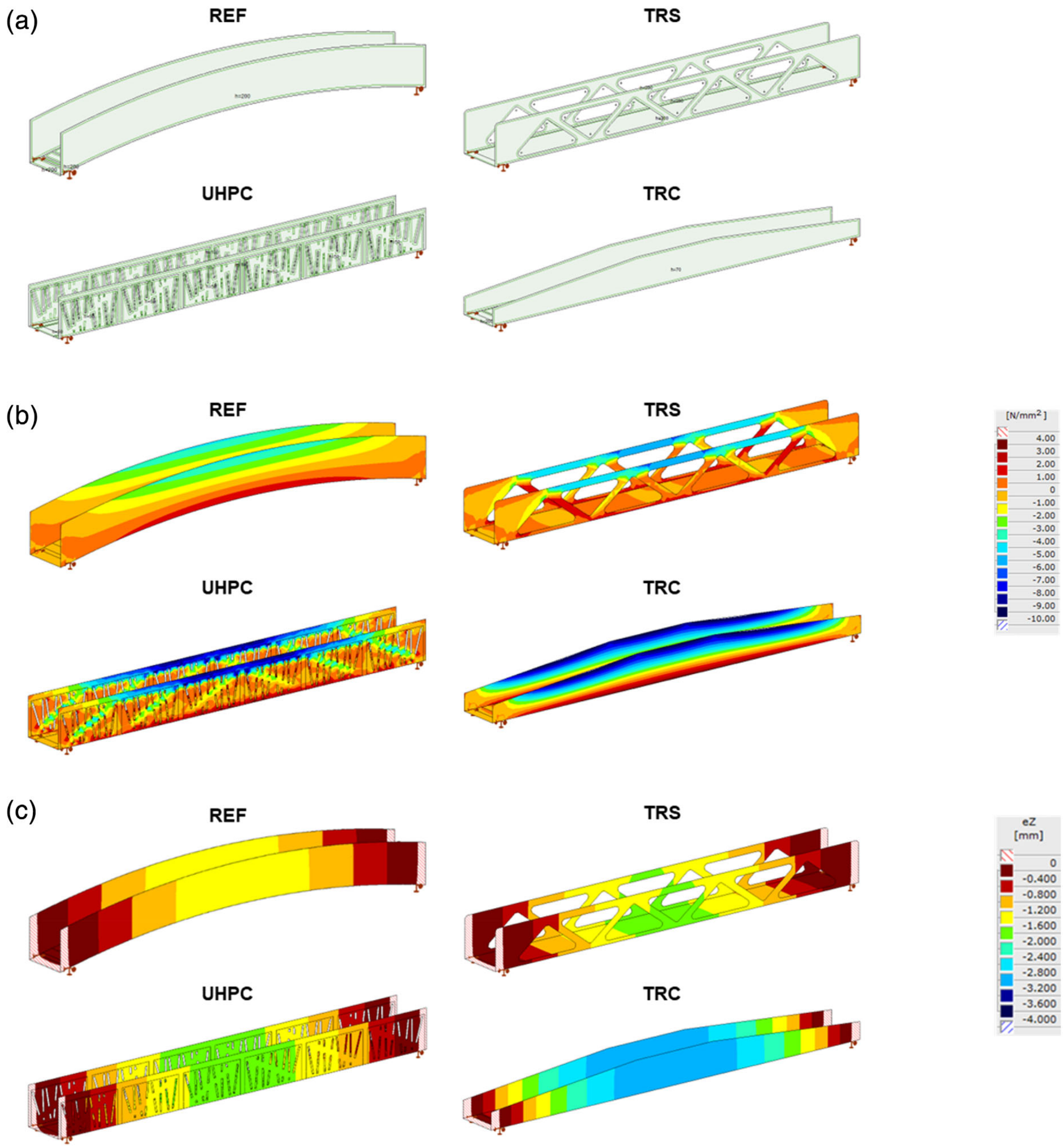


FIGURE 6 Structural analysis for the REF, TRS, UHPC, and TRC alternatives performed with AxisVM-X6: (a) finite element model; (b) principal stresses in X; and (c) vertical deformation.

the other alternatives. Figure 6 presents the finite element model (Figure 6a), the principal stresses in X (Figure 6b) and the vertical deformation (Figure 6c) for the different alternatives analyzed.

### 4.2 | Evaluation

Table 6 shows the results from the quantification of the alternatives. It presents the results for each of the six indicators corresponding to each alternative analyzed in this study. Data for Indicator 1 was provided by companies. The construction cost for the 3DPC alternative is not shown due to data confidentiality, as the information was provided by a company. For the evaluation of Indicator 2, the designs of the alternatives and their compositions, which are described above, were used. Indicators 3 and 4 were calculated using EPDs.[62–64] Lastly, Indicators 5 and 6 do not have units, as they are dimensionless indicators. They were calculated based on the literature.[27,54]

## 5 | RESULTS AND DISCUSSION

In this section, the results for the sustainability indices (SI) obtained are discussed. Then, a sensitivity analysis is presented.

### 5.1 | Sustainability indices

The results of the sustainability indices are shown in Figure 7. The five analyzed alternatives are shown in the x-axis, while the y-axis represents the global sustainability index. For each alternative, results are shown split into the three sustainability pillars, which in the graph are represented in different colors. For disaggregated results for each indicator, the reader is referred to Figure A1.

As it can be observed, the most sustainable alternative is the footbridge UHPC, which has a global sustainability index of 0.77. In this alternative, the environmental requirement is particularly high. The results for this alternative are much higher than those of the innovative technologies 3DPC and TRC, whose results are strongly affected by the high construction costs.

The second most sustainable alternative is the traditional footbridge, TRS, with a SI of 0.75. For this alternative, relatively high results are obtained for the three requirements, namely economic, environmental, and social. This footbridge is the most sustainable alternative among the most traditional methods. This shows that a well-chosen design, with optimal sections, and reducing the use of concrete not only derives in an economic benefit but also environmental.

Hence, TRS and UHPC are—for these boundary conditions—equivalent from the SI perspective since the difference ($\Delta SI = 0.02$) is negligible and within the range of the variability (due to uncertainties of the data, and other sources) of SI.

The footbridge used as a reference, REF, is the third most sustainable alternative, with a sustainability index of 0.64. This is mainly because it is the most economical footbridge among all the analyzed ones. Using a traditional alternative carries high economic benefit.

The footbridge TRC resulted with a sustainability index of 0.53. In fact, the results obtained for this alternative are almost the same as those of 3DPC. The

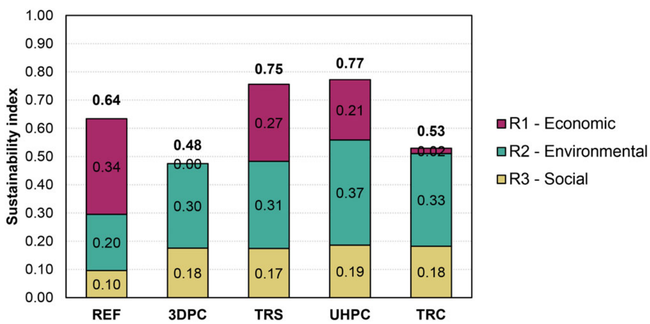


FIGURE 7 Results of the sustainability indices.

TABLE 6 Evaluation of the alternatives according to the MIVES model.

| Indicator | | Unit | Alternative REF | 3DPC | TRS | UHPC | TRC |
|---|---|---|---|---|---|---|---|
| 1 | Construction costs | € | 20,700 | * | 27,300 | 32,200 | 52,200 |
| 2 | Material consumption | t | 22.8 | 14.04 | 15.17 | 7.63 | 7.6 |
| 3 | Energy consumption | MJ | 34,067 | 22,283 | 27,217 | 11,102 | 26,153 |
| 4 | $CO_2$ emissions | kg $CO_2$-eq | 3170 | 2965 | 2479 | 2007 | 2584 |
| 5 | ORI | - | 11.914 | 5.267 | 5.511 | 2.998 | 3.843 |
| 6 | Local nuisances | - | 0.2 | 1 | 1 | 1 | 1 |

**TABLE 7** Weights allocated to the requirements in each of the sensitivity scenarios.

| Requirements | Project | Equal | Economic | Environmental | Social |
|---|---|---|---|---|---|
| $R_1$—Economic | 40% | 33.33% | 60% | 20% | 20% |
| $R_2$—Environmental | 40% | 33.33% | 20% | 60% | 20% |
| $R_3$—Social | 20% | 33.33% | 20% | 20% | 60% |

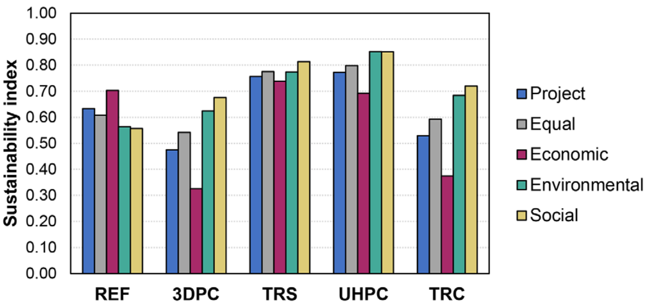


**FIGURE 8** Results of the sensitivity analysis.

*construction costs* ($R_1$) and the integration of a galvanized metallic handrail, which negatively influences the *environmental requirement* ($R_3$), lower the final index of sustainability.

Finally, the footbridge 3DPC resulted with a sustainability index of 0.48. As it can be seen, the high production cost penalizes the results of this footbridge. Nonetheless, it needs to be noted that the value of the environmental requirement is 33% higher than the value of the reference footbridge, REF (see Table 6). In fact, the 3DPC footbridge allows saving 40% of materials in comparison to the conventional alternative REF, and a 10% in comparison to footbridge TRS, in which the use of material is optimized. If compared to UHPC and TRC, the 3DPC has a material consumption that is 45% higher.

Regarding energy consumption, the 3DPC footbridge allows for a 35% reduction in energy consumption compared to the traditional solution, REF, and a 20% reduction compared to the TRS footbridge (see Table 6). Additionally, the UHPC and TRC solutions lead to lower energy consumption compared to the 3DPC. This represents up to 50% in the case of the UHPC footbridge and up to 15% in the case of the TRC footbridge.

As for $CO_2$ emissions, the 3DPC footbridge emits 10% less than the traditional REF solution (see Table 6) if the steel curve frame is considered (in fact, according to its designers, it was not necessary), while this value would increase to 25% if it is not considered. The TRS footbridge reduces emissions by 20% compared to the 3DPC footbridge, since both have the same volume of concrete, but TRS uses less cement in the concrete mix (500 kg/m$^3$ in 3DPC compared to 315 kg/m$^3$ in TRS). In addition, the UHPC footbridge reduces emissions by 30% compared to those generated by the 3DPC footbridge since, despite having a 50% lower concrete volume, it has a higher dosage of concrete (750 kg/m$^3$). Instead, the TRC footbridge, with a 50% lower concrete volume and the same cement dosage (500 kg/m$^3$) as the 3DPC footbridge, increases emissions by 10% due to the production of the galvanized steel railing.

From the perspective of social impacts, the two innovative footbridges reduce occupational risk by more than 30% compared to the 3DPC footbridge, and all prefabricated footbridges produce less risks than the one cast in place, REF. Similarly, the footbridges that are precast and dry-jointed generate less disturbance to third parties than the cast-in-place REF footbridge.

### 5.2 | Sensitivity analysis

The results presented above are based on a collection of weights assigned using the case studies of sustainability assessments of civil engineering and architecture case studies. Nevertheless, this set of weights may not be representative of all decision-makers, which can change with time, geographical location, culture, etc. Therefore, this section presents a sensitivity analysis where the different weights are changed and the impact of these changes on the sustainability indices are examined.

The four scenarios defined are presented in Table 7 and are: (1) equal weights, (2) economic weight being three times higher than the other two requirements, (3) environmental weight being three times higher than the other two requirements, and (4) social weight being three times higher than the other two requirements.

The results of the sensitivity analysis (see Figure 8) show that, in most of the scenarios analyzed, the footbridge UHPC is the one with the highest sustainability index, which confirms the results presented in the previous section. An exception to this is the economic scenario, where the footbridge built using traditional methods is the most efficient one.

## 6 | CONCLUSIONS

This article focused on the assessment of the sustainability of concrete footbridges, including the 3DPC technology as an alternative. The main goal of this paper is to present an approach for assessing sustainability index of short-span footbridges (span inferior to 20 m). In this regard, the method developed provides engineers and designers with an approach for decision-making based on sustainability performance.

For this purpose, a comparative analysis was conducted among two traditional concrete solutions, namely a cast-in-place reinforced concrete solution with closed parapets (REF) and a precast concrete truss solution (TRS), along with two technologically innovative solutions: a precast ultra-high performance concrete solution (UHPC) and a precast textile reinforced concrete solution (TRC). These designs were benchmarked against a 3DPC alternative.

For the economic requirement, the highest sustainability index is obtained by the REF footbridge, followed by the TRS. This result proves that—partly due to their competitive manufacturing cost—classical solutions should not be discarded from the beginning as a feasible solution and, besides, under an optimized design, they still have several advantages in terms of sustainability.

The findings revealed that, for the boundary conditions considered, the economic sustainability of the 3DPC alternative was suboptimal. 3DPC technology is currently under development and, consequently, a direct comparison with other mature technologies established in the market would not provide a representative view from the sustainability perspective. From an economic point of view, the 3DPC solution is penalized by its manufacturing costs, which nowadays prevents this solution from being competitive within the current construction market economic requirements and competitiveness. It must be remarked, nonetheless, that this outcome does not—and should not—preclude the possibility that, with advances in this technology and with a reduction in manufacturing costs, this alternative could be more sustainable (and even more so than existing alternatives) in the near future. In fact, as the maturity degree of the technology increases, costs are expected to decrease and the economic performance to increase accordingly.

In this sense, maintaining the weights' set and considering the environmental and social satisfactions independent of the economic requirement, the cost of the 3DPC footbridge analyzed should not exceed 1.8× the cost of the REF solution to achieve an equivalent sustainability performance ($SI = 0.63$). Likewise, for achieving an SI equivalent to that of the UHPC ($SI = 0.77$), the cost should be 1.3× with respect to the cost of the REF.

In terms of the environmental and social requirements, for this case study, the 3DPC footbridge led to higher environmental and social performances respect to those achieved by the traditional solutions analyzed, but lower than those technologically innovative alternatives identified and included in this research. This underscores the possibilities that exist for 3DPC technology in enhancing sustainability aspects through, for instance, increased resource use efficiency and improved safety conditions.

This being said, one of the limitations of this study was the availability of data. As digital fabrication with cement-based materials applied to footbridges is a recent technology, there is not enough data available to evaluate the evolution of the behavior of the properties of the mortar-cement base material over time, and aspects such as durability of the mortars (and its reinforcement, when necessary) are unknown, yet. Additionally, while the approach proposed to assess the sustainability performance of footbridges might be useful for other case studies, the results and conclusions derived for the DFC footbridge studied herein should not be generalized and extended to other DFC-based components.

## ACKNOWLEDGMENTS

The authors want to acknowledge ACCIONA, S.A. for the economic funds and information provided. This study was also financially supported by the Spanish Ministry of Science and Innovation under the scope of project CREEF (PID2019-108978RB-C32/AEI/10.13039/501100011033).

A. Monserrat was supported by the Ministerio de Universidades (Spain) with the Recovery, Transformation and Resilience Plan (RD 289/2021 and order UNI/551/2021) of NextGenerationEU; Postdoctoral Margarita Salas Fellowship funded by Universitat Politècnica de València.

## DATA AVAILABILITY STATEMENT

The data that support the findings of this study are available on request from the corresponding author. The data are not publicly available due to privacy or ethical restrictions.

## ORCID

*Javier Asensio* https://orcid.org/0000-0002-0558-6149
*Irene Josa* https://orcid.org/0000-0002-1538-4567
*Andrea Monserrat* https://orcid.org/0000-0002-1480-4021
*Albert de la Fuente* https://orcid.org/0000-0002-8016-1677

## REFERENCES

1. Flatt RJ, Wangler T. On sustainability and digital fabrication with concrete. Cem Concr Res. 2022;158:106837. https://doi.org/10.1016/j.cemconres.2022.106837
2. García de Soto B, Agustí-Juan I, Hunhevicz J, Joss S, Graser K, Habert G, et al. Productivity of digital fabrication in construction: cost and time analysis of a robotically built wall. Autom

Constr. 2018;92:297–311. https://doi.org/10.1016/j.autcon.2018.04.004

3. Kloft H, Krauss HW, Hack N, Herrmann E, Neudecker S, Varady PA, et al. Influence of process parameters on the interlayer bond strength of concrete elements additive manufactured by Shotcrete 3D Printing (SC3DP). Cem Concr Res. 2020;134:106078. https://doi.org/10.1016/j.cemconres.2020.106078
4. Bhattacherjee S, Basavaraj AS, Rahul AV, Santhanam M, Gettu R, Panda B, et al. Sustainable materials for 3D concrete printing. Cem Concr Compos. 2021;122:104156. https://doi.org/10.1016/j.cemconcomp.2021.104156
5. Zhang N, Xia M, Sanjayan J. Short-duration near-nozzle mixing for 3D concrete printing. Cem Concr Res. 2022;151:106616. https://doi.org/10.1016/j.cemconres.2021.106616
6. Li Z, Ma G, Wang F, Wang L, Sanjayan J. Expansive cementitious materials to improve micro-cable reinforcement bond in 3D concrete printing. Cem Concr Compos. 2022;125:104304. https://doi.org/10.1016/j.cemconcomp.2021.104304
7. Marchment T, Sanjayan J. Bond properties of reinforcing bar penetrations in 3D concrete printing. Autom Constr. 2020;120:103394. https://doi.org/10.1016/j.autcon.2020.103394
8. Buswell RA, da Silva WRL, Bos FP, Schipper HR, Lowke D, Hack N, et al. A process classification framework for defining and describing Digital Fabrication with Concrete. Cem Concr Res. 2020;134:106068. https://doi.org/10.1016/j.cemconres.2020.106068
9. Weger D, Talke D, Lowe D, Henke K. 3D-Betondruck, Variante 'Paste intrusion'. *Herstellung Eines Mit Inneren Streben Ausgesteiften Rohres*. Gefördert Durch Informationszentrum Beton GmbH. 2017.
10. Khoshnevis B, Hwang D, Yao K-T, Yeh Z, Khoshnevis B, Hwang D, et al. Mega-scale fabrication by contour crafting. Int J Ind Syst Eng. 2006;1(3):301.
11. Jakupovic A. D-shape—report. 2016.
12. Ma G, Buswell R, Leal da Silva WR, Wang L, Xu J, Jones SZ. Technology readiness: a global snapshot of 3D concrete printing and the frontiers for development. Cem Concr Res. 2022;156:106774. https://doi.org/10.1016/j.cemconres.2022.106774
13. Khoshnevis B. Automated construction by contour crafting—related robotics and information technologies. Autom Constr. 2004;13(1):5–19. https://doi.org/10.1016/j.autcon.2003.08.012
14. Hager I, Golonka A, Putanowicz R. 3D printing of buildings and building components as the future of sustainable construction? Procedia Eng. 2016;151:292–9. https://doi.org/10.1016/j.proeng.2016.07.357
15. Perkins I, Skitmore M. Three-dimensional printing in the construction industry: a review. Int J Constr Manag. 2015;15(1):1–9. https://doi.org/10.1080/15623599.2015.1012136
16. Lowke D, Dini E, Perrot A, Weger D, Gehlen C, Dillenburger B. Particle-bed 3D printing in concrete construction—possibilities and challenges. Cem Concr Res. 2018;112:50–65. https://doi.org/10.1016/j.cemconres.2018.05.018
17. Lowke D, Mai I, Keita E, Perrot A, Weger D, Gehlen C, et al. Material-process interactions in particle bed 3D printing and the underlying physics. Cem Concr Res. 2022;156:106748. https://doi.org/10.1016/j.cemconres.2022.106748
18. Lowke D, Talke D, Dressler I, Weger D, Gehlen C, Ostertag C, et al. Particle bed 3D printing by selective cement activation—applications, material and process technology. Cem Concr Res. 2020;134:106077. https://doi.org/10.1016/j.cemconres.2020.106077
19. Pierre A, Weger D, Perrot A, Lowke D. Additive manufacturing of cementitious materials by selective paste intrusion: numerical modeling of the flow using a 2d axisymmetric phase field method. Materials. 2020;13(21):1–15. https://doi.org/10.3390/ma13215024
20. Ingaglio J, Fox J, Naito CJ, Bocchini P. Material characteristics of binder jet 3D printed hydrated CSA cement with the addition of fine aggregates. Construct Build Mater. 2019;206:494–503. https://doi.org/10.1016/j.conbuildmat.2019.02.065
21. Ma GW, Wang L, Ju Y. State-of-the-art of 3D printing technology of cementitious material—an emerging technique for construction. Sci China Technol Sci. 2018;61(4):475–95. https://doi.org/10.1007/s11431-016-9077-7
22. Menna C, Mata-Falcón J, Bos FP, Vantyghem G, Ferrara L, Asprone D, et al. Opportunities and challenges for structural engineering of digitally fabricated concrete. Cem Concr Res. 2020;133:106079. https://doi.org/10.1016/j.cemconres.2020.106079
23. huaxia. 3D-printed concrete bridge unveiled in North China. Xinhua. 2019 Available from: http://www.xinhuanet.com/english/2019-10/15/c_138474114.htm
24. XtreeE. Pedestrian footbridge in Aubervilliers (project). The Large-Scale 3D. 2020 Available from: https://xtreee.com/en/project/pedestrian-footbridge-in-aubervilliers-greater-paris-france/
25. Agustí-Juan I, Müller F, Hack N, Wangler T, Habert G. Potential benefits of digital fabrication for complex structures: environmental assessment of a robotically fabricated concrete wall. J Clean Prod. 2017;154:330–40. https://doi.org/10.1016/j.jclepro.2017.04.002
26. Khan MS, Sanchez F, Zhou H, 3-D printing of concrete: beyond horizons, Cem. Concr. Res. 2020;133:106070. https://doi.org/10.1016/j.cemconres.2020.106070
27. de la Fuente A, Blanco A, Galeote E, Cavalaro S. Structural fibre-reinforced cement-based composite designed for particle bed 3D printing systems. Case study Parque de Castilla footbridge in Madrid. Cem Concr Res. 2022;157:106801. https://doi.org/10.1016/j.cemconres.2022.106801
28. Boix-Cots D, Pardo-Bosch F, Blanco A, Aguado A, Pujadas P. A systematic review on MIVES: a sustainability-oriented multi-criteria decision-making method. Build Environ. 2022;223:109515. https://doi.org/10.1016/j.buildenv.2022.109515
29. Josa I, Pons O, de la Fuente A, Aguado A. Multi-criteria decision-making model to assess the sustainability of girders and trusses: case study for roofs of sports halls. J Clean Prod. 2020;249:119312. https://doi.org/10.1016/j.jclepro.2019.119312
30. del Mar Casanovas-Rubio M, Pujadas P, Pardo-Bosch F, Blanco A, Aguado A. Sustainability assessment of trenches including the new eco-trench: a multi-criteria decision-making tool. J Clean Prod. 2019;238:117957. https://doi.org/10.1016/j.jclepro.2019.117957
31. de la Fuente A, Blanco A, Armengou J, Aguado A. Sustainability based-approach to determine the concrete type and reinforcement configuration of TBM tunnels linings. Case study: extension line to Barcelona airport T1. Tunn Undergr Space Technol. 2017b;61:179–88. https://doi.org/10.1016/j.tust.2016.10.008

32. Ormazabal G, Viñolas B, Aguado A. Enhancing value in crucial decisions: line 9 of the Barcelona Subway. J Manag Eng. 2008; 24(4):265–72. https://doi.org/10.1061/(ASCE)0742-597X(2008)24:4(265)
33. De La Fuente A, Blanco A, Henrique S, Cavalaro P, Aguado A. Sustainability assessment of different reinforcement alternatives for precast concrete segmental linings. 2016 Available from: https://www.researchgate.net/publication/304524593
34. de la Fuente A, Pons O, Josa A, Aguado A. Multi-criteria decision making in the sustainability assessment of sewerage pipe systems. J Clean Prod. 2016;112:4762–70. https://doi.org/10.1016/j.jclepro.2015.07.002
35. Pardo-Bosch F, Aguado A. Investment priorities for the management of hydraulic structures. Struct Infrastruct Eng. 2015; 11(10):1338–51. https://doi.org/10.1080/15732479.2014.964267
36. Cartelle Barros JJ, Lara Coira M, de la Cruz López MP, del Caño Gochi A. Assessing the global sustainability of different electricity generation systems. Energy. 2015;89:473–89. https://doi.org/10.1016/j.energy.2015.05.110
37. Pons O, Aguado A. Integrated value model for sustainable assessment applied to technologies used to build schools in Catalonia, Spain. Build Environ. 2012;53:49–58. https://doi.org/10.1016/j.buildenv.2012.01.007
38. Pons O, De La Fuente A. Integrated sustainability assessment method applied to structural concrete columns. Construct Build Mater. 2013;49:882–93. https://doi.org/10.1016/j.conbuildmat.2013.09.009
39. Reyes JP, San-José JT, Cuadrado J, Sancibrian R. Health & Safety criteria for determining the sustainable value of construction projects. Saf Sci. 2014;62:221–32. https://doi.org/10.1016/j.ssci.2013.08.023
40. Sánchez-Garrido AJ, Yepes V. Multi-criteria assessment of alternative sustainable structures for a self-promoted, single-family home. J Clean Prod. 2020;258:120556. https://doi.org/10.1016/j.jclepro.2020.120556
41. San-José Lombera J-T, Cuadrado Rojo J. Industrial building design stage based on a system approach to their environmental sustainability. Construct Build Mater. 2010;24(4):438–47. https://doi.org/10.1016/j.conbuildmat.2009.10.019
42. San-José Lombera J-T, Garrucho Aprea I. A system approach to the environmental analysis of industrial buildings. Build Environ. 2010;45(3):673–83. https://doi.org/10.1016/j.buildenv.2009.08.012
43. Hosseini SMA, Albert, de la F, Oriol P. Multicriteria decision-making method for sustainable site location of post-disaster temporary housing in urban areas. J Constr Eng Manag. 2016; 142(9):4016036. https://doi.org/10.1061/(ASCE)CO.1943-7862.0001137
44. Hosseini SMA, de la Fuente A, Pons O. Multi-criteria decision-making method for assessing the sustainability of post-disaster temporary housing units technologies: a case study in Bam, 2003. Sustain Cities Soc. 2016;20:38–51. https://doi.org/10.1016/j.scs.2015.09.012
45. del Caño A, de la Cruz MP, Gómez D, Pérez M. Fuzzy method for analysing uncertainty in the sustainable design of concrete structures. J Civ Eng Manag. 2016;22(7):924–35. https://doi.org/10.3846/13923730.2014.928361
46. del Caño A, Gómez D, de la Cruz MP. Uncertainty analysis in the sustainable design of concrete structures: a probabilistic method. Construct Build Mater. 2012;37:865–73. https://doi.org/10.1016/j.conbuildmat.2012.04.020
47. Bos FP, Ahmed ZY, Jutinov ER, Salet TAM. Experimental exploration of metal cable as reinforcement in 3D printed concrete. Materials. 2017;10(11):1–22. https://doi.org/10.3390/ma10111314
48. Salet TAM, Ahmed ZY, Bos FP, Laagland HLM. Design of a 3D printed concrete bridge by testing*. Virtual Phys Prototyp. 2018;13(3):222–36. https://doi.org/10.1080/17452759.2018.1476064
49. Tsinghua University. The world's largest concrete 3D printed pedestrian bridge. School of Architecture. 2019 Available from: https://www.tsinghua.edu.cn/en/info/1244/2966.htm
50. Valdivieso R. Sostenibilidad en el Sector de la Construcción. Sostenibilidad en Estructuras y Puentes Ferroviarios. Universidad Politécnica de Madrid. 2016.
51. Pons O, Casanovas-Rubio MM, Armengou J, de la Fuente A. Sustainability-driven decision-making model: case study of fiber-reinforced concrete foundation piles. J Constr Eng Manag. 2021;147(10). https://doi.org/10.1061/(asce)co.1943-7862.0002073
52. Fédération International du Béton (fib). Sustainability of precast structures. State of the art report. 2018.
53. de la Fuente A, Armengou J, Pons O, Aguado A. Multi-criteria decision-making model for assessing the sustainability index of wind-turbine support systems: application to a new precast concrete alternative. J Civ Eng Manag. 2017a;23(2):194–203. https://doi.org/10.3846/13923730.2015.1023347
54. del Mar Casanovas M, Armengou J, Ramos G. Occupational risk index for assessment of risk in construction work by activity. J Constr Eng Manag. 2014;140(1). https://doi.org/10.1061/(asce)co.1943-7862.0000785
55. EN 1992-1-1. Eurocode 2: Design of concrete structures—Part 1-1: general rules and rules for buildings. 2004.
56. Institute for advance architecture of Catalonia [IAAC]. 3D printed bridge. n.d. [cited 2022 Nov 26]. Available from: https://iaac.net/project/3d-printed-bridge/
57. Serna P, López J, Coll H, Camacho E, Navarro-Gregori J, Galán F. Pasarela de hormigón de muy alto rendimiento sobre el Barranco de las Ovejas (Alicante). Hormigón y Acero. 2015; 66:23–42. https://doi.org/10.1016/j.hya.2014.12.001
58. Sollertia—Groupe d'Ingenieurs. Passerelle en BFUP au Bouveret. Civil Engineering, Environment and Public Works. 2018 Available from: https://sollertia.ch/portfolio/passerelle-en-bfup-au-bouveret/
59. Teixeira R, Laurencet P, Brühwiler E. Passerelle intégrale en CFUP armé et précontraint au Bouveret. 3ème Journée d'étude, 24 Octobre 2019 BÉTON FIBRÉ ULTRA-PERFORMANT Concevoir, Dimensionner, Construire, 169–178. 2019 Available from: http://infoscience.epfl.ch/record/275990
60. knippershelbig. Modular textile-concrete bridge. Projects. 2015 Available from: https://www.knippershelbig.com/en/projects/modular-textile-concrete-bridge
61. Rempel S, Kulas C, Will N, Bielak J. Extremely light and slender precast pedestrian-bridge made out of textile-reinforced concrete (TRC). In DA Hordijk, M Luković, eds., High tech concrete: where technology and engineering meet; Maastricht: Springer Cham; 2018. p. 2530–7. https://doi.org/10.1007/978-3-319-59471-2_288

62. InformationsZentrum Beton GmbH. Environmental product declaration for Beton C 30/37. Declaration number: EPD-IZB-20180102-IBG1-DE; Institut Bauen und Umwelt e.V. (IBU). 2018a.
63. InformationsZentrum Beton GmbH. Environmental product declaration for Beton C 35/45. Declaration number: EPD-IZB-20180098-IBG1-DE; Institut Bauen und Umwelt e.V. (IBU). 2018b.
64. InformationsZentrum Beton GmbH. Environmental product declaration for Beton C 50/60. Declaration number: EPD-IZB-20180100-IBG1-DE; Institut Bauen und Umwelt e.V. (IBU). 2018c.


## AUTHOR BIOGRAPHIES

**Javier Asensio**, WMM Ingenieure AG, Münchenstein, Switzerland. Email: j.asensio@wmm.ch.

**Irene Josa**, Department of Civil, Environmental & Geomatic Engineering, University College London, London, UK. Email: i.josa@ucl.ac.uk.

**Andrea Monserrat**, Department of Civil and Environmental Universitat Politècnica de Catalunya (UPC) Postdoctoral Margarita Salas Fellowship funded by Universitat Politècnica de València, Barcelona, Spain. Email: andrea.monserrat@upc.edu.

**Albert de la Fuente**, Department of Civil and Environmental Engineering, Universitat Politècnica de Catalunya (UPC), Barcelona, Spain. Email: albert.de.la.fuente@upc.edu.

**How to cite this article:** Asensio J, Josa I, Monserrat A, de la Fuente A. 3D-printed concrete footbridges: An approach to assess the sustainability performance. Structural Concrete. 2023. https://doi.org/10.1002/suco.202201227

## APPENDIX

The article reviewed various studies to gain insights into the application of weights in decision-making trees. Specifically, articles focusing on the following structural elements or infrastructures were examined: bridges,[50] pilots,[51] roofs,[29] prefabricated structures,[52] tunnels,[33,34] and wind turbines.[31,53] The mean weight and coefficient of variance for different aspects were calculated and utilized as described below.

Analyzing the averages and deviations of the weights for the requirements (as presented in Table A1), it is evident that both the economic (37.0%) and environmental (38.3%) requirements hold equal significance in assessing the sustainability of infrastructures. The social requirement, on the other hand, carries a relatively lower weight of 24.5%.

In terms of the criteria, Table A2 reveals that construction cost (24.1%) emerges as the most significant criterion, with a weight considerably higher (around 50%) than emissions (13.6%) and material and resource consumption (13.2%). Table A2 underscores the criteria with weights around 10% or higher as the most representative, as they appear most frequently in the presented cases. These criteria were taken into account in configuring the proposed decision tree.

Lastly, in terms of indicators, the construction cost (20.5%) holds the highest relative weight, which is 60% higher than the emissions indicator (12.8%). Table A3 emphasizes the indicators with weights around or above

**TABLE A1** Statistical analysis of requirements and allocated weights.

| Requirements | Bridges | Pilots | Roofs | Prefab. struct. | Tunnels | Wind turbines | Mean | CoV |
|---|---|---|---|---|---|---|---|---|
| Economic | 40% | 43.8% | 30% | 35% | 40% | 33.3% | 37.0% | −14% |
| Environmental | 45% | 28.7% | 40% | 38% | 45% | 33.3% | 38.3% | −17% |
| Social | 15% | 27.5% | 30% | 26% | 15% | 33.3% | 24.5% | −32% |

**TABLE A2** Statistical analysis of criteria and allocated weights.

| Criteria | Bridges | Pilots | Roofs | Prefab. struct. | Tunnels | Wind turbines | Mean | CoV |
|---|---|---|---|---|---|---|---|---|
| *Economic* | | | | | | | | |
| Construction cost | 28.00% | 30.10% | 22.50% | 14.70% | 36.00% | 13.30% | 24.10% | −37% |
| Maintenance cost | 12.00% | - | 7.50% | - | 4.00% | 13.30% | 6.10% | −94% |
| Construction time | - | 13.70% | - | - | - | - | 2.30% | -% |
| Quality | - | - | - | 6.70% | - | - | 1.10% | -% |
| Demolition | - | - | - | 3.20% | - | 6.70% | 1.60% | -% |
| Service life | - | - | - | 10.50% | - | - | 1.80% | -% |
| *Environmental* | | | | | | | | |
| Resource consumption | 18.00% | 6.30% | 13.30% | 16.70% | 13.50% | 11.10% | 13.20% | −32% |
| Emissions | 6.80% | 13.70% | 20.00% | 12.20% | 18.00% | 11.10% | 13.60% | −35% |
| Waste | 6.80% | - | - | - | - | - | 1.10% | -% |
| Energy | 4.50% | 8.70% | 6.70% | 9.10% | 13.50% | 11.10% | 8.90% | −36% |
| Environmental management | 9.00% | - | - | - | - | - | 1.50% | -% |
| *Social* | | | | | | | | |
| Local community | 12.80% | - | - | - | - | - | 2.10% | -% |
| Resilience | 2.30% | - | - | - | - | - | 0.40% | -% |
| Occupational risk (security) | - | 13.80% | 9.00% | 16.40% | 15.00% | 10.00% | 10.70% | −56% |
| Third party effects | - | 7.20% | - | 9.60% | - | - | 2.80% | -% |
| Innovation | - | 6.50% | - | - | - | - | 1.10% | -% |
| Perception | - | - | 21.00% | - | - | 20.00% | 6.80% | -% |
| Technological integration | - | - | - | - | - | 3.30% | 0.60% | -% |

TABLE A3 Statistical analysis of indicators and allocated weights.

| Indicators | Bridges | Pilots | Roofs | Prefab. struct. | Tunnels | Wind turbines | Mean | CoV |
|---|---|---|---|---|---|---|---|---|
| *Economic* | | | | | | | | |
| Construction cost | 23.8% | 12.5% | 22.5% | 14.7% | 36.0% | 13.3% | 20.5% | 44% |
| Maintenance/service costs | 10.8% | 11.4% | 7.5% | 6.4% | 4.0% | 13.3% | 8.9% | 39% |
| ISO 9001 | 4.2% | - | - | - | - | - | 0.7% | -% |
| Resilience | 1.2% | - | - | 4.1% | - | - | 0.9% | -% |
| Construction time | - | 13.7% | - | - | - | - | 2.3% | -% |
| Quality costs | - | 6.2% | - | 6.7% | - | - | 2.1% | -% |
| Demolition | - | - | - | 3.2% | - | 6.7% | 1.6% | -% |
| *Environmental* | | | | | | | | |
| Consumption of natural resources | 10.8% | - | 6.7% | 12.4% | 10.8% | 11.1% | 8.6% | 54% |
| Water use | 2.7% | 6.3% | 6.7% | 2.0% | 2.7% | - | 3.4% | 76% |
| Use of recycled resources | 4.5% | - | - | 2.3% | - | - | 1.1% | -% |
| Emissions | 6.8% | 13.7% | 20.0% | 7.5% | 18.0% | 11.1% | 12.8% | 42% |
| Waste | 6.8% | - | - | 4.6% | - | - | 1.9% | -% |
| Energy | 4.5% | 8.7% | 6.7% | 9.1% | 13.5% | 11.1% | 8.9% | 36% |
| Ecological value | 6.3% | - | - | - | - | - | 1.1% | -% |
| ISO 14001 | 2.7% | - | - | - | - | - | 0.5% | -% |
| *Social* | | | | | | | | |
| Public information | 2.6% | - | - | - | - | - | 0.4% | -% |
| Local employment | 5.1% | - | - | - | - | - | 0.9% | -% |
| Occupational risk during construction | - | 13.8% | 6.3% | 7.5% | 4.5% | 10.0% | 7.0% | 67% |
| Risk during service | - | - | 2.7% | 9.0% | - | - | 2.0% | -% |
| Third party effects | 5.1% | - | 3.2% | - | - | - | 1.4% | -% |
| Acoustic pollution | - | - | - | 1.4% | 10.5% | - | 2.0% | -% |
| Dust pollution | - | - | - | 1.9% | - | - | 0.3% | -% |
| Traffic disturbance | - | - | - | 1.3% | - | - | 0.2% | -% |
| Space during construction | - | 7.2% | - | - | - | - | 1.2% | -% |
| User comfort | - | - | 11.6% | 5.0% | - | - | 2.8% | -% |
| Traffic stoppage | 2.3% | - | - | - | - | - | 0.4% | -% |
| New solutions/patents | - | 6.5% | - | - | - | 3.3% | 1.6% | -% |
| Adaptability | - | - | 3.2% | - | - | - | 0.5% | -% |
| Installations | - | - | 3.2% | - | - | - | 0.5% | -% |
| Proportions | - | - | - | - | - | 10.0% | 1.7% | -% |
| Flexibility | - | - | - | - | - | 10.0% | 1.7% | -% |

5%. These indicators are considered the most representative and were the ones incorporated into the configuration of the decision tree.

Table A4 includes the parameters used to define indicator $I_6$, local nuisances.

Figure A1 shows the value functions used in each indicator, as well as the quantification of the indicators for each alternative. On the x-axis, the value of the non-normalized indicators is shown. The y-axis corresponds to the value of the indicator after applying the value function.

**TABLE A4** Definition of the scale for indicator $I_6$, local nuisances.

| Value of the indicator | Description |
|---|---|
| 0.2 | Very high number of equipment is needed, and there is in situ concrete casting. |
| 0.4 | High number of equipment is needed, and there is self-compacting concrete casting in situ. |
| 0.6 | Equipment and operations to cast concrete in the joints and to move heavy precast elements (of density above 1000 $kg/m^3$) are needed. |
| 0.8 | Equipment and operations to cast concrete in the joints and to move light precast elements (of density below 1000 $kg/m^3$) are needed. |
| 1.0 | There are only dry or none connections needed in the precast elements. |

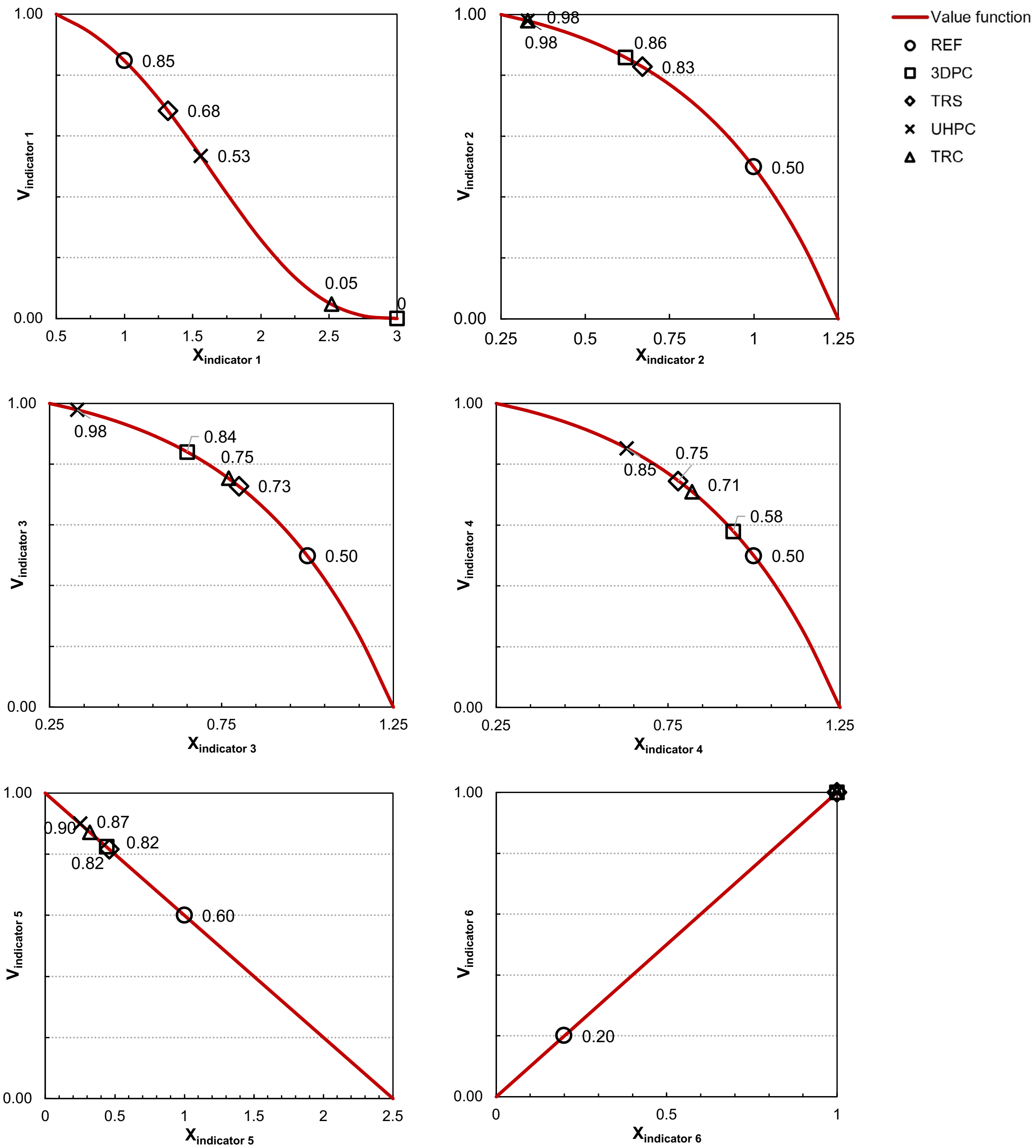


**FIGURE A1** Value functions and results for each alternative of the case study.